*Journal of Fluids and Structures* (2001) **15,** 133–150
doi:10.1006/jfls.2000.0328, available online at http://www.idealibrary.com on IDEAL®

# LOW-FREQUENCY RESPONSES OF NONLINEARLY MOORED VESSELS IN RANDOM WAVES: COUPLED SURGE, PITCH AND HEAVE MOTIONS

A. Sarkar and R. Eatock Taylor

*Department of Engineering Science, University of Oxford*
*Parks Road, Oxford OX1 3PJ, U.K.*

(Received 2 October 1998, and in final form 20 June 2000)

The responses of a multi-degree-of-freedom model of a moored vessel are analysed, accounting for the hydroelastic interaction between the nonlinear wave hydrodynamics and the nonlinear mooring stiffness. A two-scale perturbation method developed by Sarkar & Eatock Taylor to determine low-frequency hydrodynamic forces on a single-degree-of-freedom model of a nonlinearly moored vessel has been extended to analyse the nonlinear multi-degree-of-freedom dynamics of the system. Surge, heave and pitch motions are considered. The perturbation equations of successive orders are derived. To illustrate the approach, semi-analytical expressions for the higher-order hydrodynamic force components have been obtained for a truncated circular cylinder in finite water depth. In addition to conventional quadratic force transfer functions, a new type of higher-order force transfer function is introduced. This is used to characterize the hydrodynamic forces on the vessel which arise due to nonlinearity of the mooring stiffness. These are a type of radiation force, generated by the nonlinear interaction of the fluid–structure coupled system. Based on a Volterra series model, the power spectral densities of the new higher-order forces are then derived for the case of Gaussian random seas. It is shown that the additional response arising due to nonlinear dynamics of the mooring system can significantly contribute to low-frequency drift forces and responses of the vessel. Unlike conventional non-Gaussian second-order forces which are quadratic transformations of a Gaussian random process, the new higher-order forces arising due to the nonlinear mooring stiffness are polynomials of a Gaussian random process (up to fourth order for a Duffing oscillator model). This may significantly influence the extreme responses.


## 1. INTRODUCTION

Typically, some moored floating structures such as semi-submersibles and catenary moored tankers show significant nonlinearity in their restoring characteristics. In the traditional design and analysis procedure, a single-scale Stokes perturbation expansion taken to second order in wave steepness is used to study the nonlinear hydrodynamic interaction which leads to low-frequency drift forces. This technique inherently assumes that the mooring stiffness is linear. In a recent paper (Sarkar & Eatock Taylor 1998), it is pointed out that the nonlinear dynamics of the vessel can significantly influence the low-frequency surge force arising due to nonlinear wave–body interactions. The two-scale perturbation technique developed in that paper for a single-degree-of-freedom model has been extended here to analyse the coupled surge, heave and pitch motions of the vessel restrained by a weakly nonlinear mooring system.

As a specific example, the low-frequency forces and responses of a truncated cylinder have been studied. The simple geometry of the structure permits a semi-analytical solution. It is

0889–9746/01/010133 + 18 $35.00/0 

shown that the low-frequency components of the surge force and pitch moment are significantly influenced by the additional first-order response of the vessel arising due to the effect of nonlinear mooring stiffness.

## 2. GOVERNING EQUATIONS AND BOUNDARY CONDITIONS

A floating vessel undergoing oscillations in surge ($\alpha$), heave ($\beta$) and pitch ($\psi$) motions due to wave actions is considered, as shown in Figure 1. Assuming potential flow theory, the fluid motion is described by the velocity potential $\varphi(x, y, z, t)$ which satisfies Laplace's equation and the usual no flow boundary condition at the sea-bottom. The combined kinematic and dynamic free surface boundary condition on $z = 0$ is given by

$$\varphi_{tt} + g\varphi_z = -2\nabla\varphi \cdot \nabla\varphi_t + \frac{1}{g}\varphi_t(\varphi_{tt} + g\varphi_z)_z + \mathcal{O}(\delta^3), \tag{1}$$

where $\delta$ is the wave steepness.

To obtain the kinematic boundary condition at the oscillating body surface $S_0$, two sets of axes are defined [following Ogilvie (1983)]: the inertial axes and the body-fixed axes. The position vector of a point in space is given by $\mathbf{X}$ and $\mathbf{X}'$ in the inertial and the body-fixed axes, respectively. It can then be shown that the kinematic boundary condition at the body surface is (Ogilvie 1983)

$$\begin{aligned}\mathbf{n}' \cdot \nabla\varphi = \mathbf{n}' \cdot \{[\boldsymbol{\xi}_t + \boldsymbol{\Psi}_t \times \mathbf{X}'] + \mathbf{H}_t \mathbf{X}' - [(\boldsymbol{\xi} + \boldsymbol{\Psi} \times \mathbf{X}') \cdot \nabla]\nabla\varphi\} \\ + (\boldsymbol{\Psi} \times \mathbf{n}') \cdot [(\boldsymbol{\xi}_t + \boldsymbol{\Psi}_t \times \mathbf{X}') - \nabla\varphi] + \mathcal{O}(\delta^3) \quad \text{on } S_m,\end{aligned} \tag{2}$$

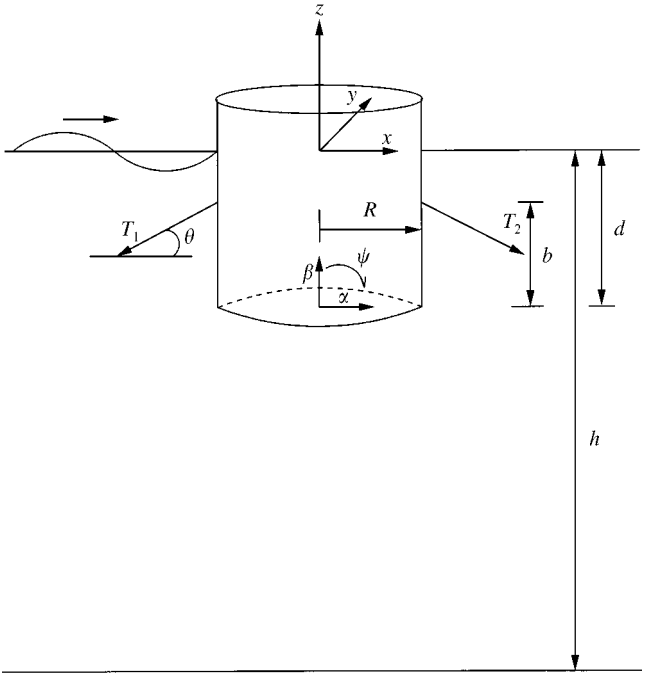


Figure 1. Physical diagram and coordinate system of a truncated cylinder.

where $\mathbf{n}'$ denotes the direction cosine vector on the body surface in the body-fixed axes. The same vector is denoted by $\mathbf{n}$ in the inertial axes. $S_m$ is the mean wetted surface of the body in its equilibrium position. The vectors $\boldsymbol{\xi}$ and $\boldsymbol{\Psi}$ and matrix $\mathbf{H}$ are given by

$$\boldsymbol{\xi} = \begin{Bmatrix} \alpha \\ 0 \\ \beta \end{Bmatrix}, \quad \boldsymbol{\Psi} = \begin{Bmatrix} 0 \\ \psi \\ 0 \end{Bmatrix}, \quad \mathbf{H} = -\frac{1}{2}\begin{bmatrix} \psi^2 & 0 & 0 \\ 0 & 0 & 0 \\ 0 & 0 & \psi^2 \end{bmatrix}.$$

The zero-mean dynamic response vector is defined as $\mathbf{A}$. The response is also assumed to have a mean $\bar{\mathbf{A}}$ due to nonlinear effects. Furthermore, an offset $\bar{\mathbf{A}}_s$ accounts for the effects of wind and current. The vectors $\mathbf{A}$, $\bar{\mathbf{A}}$ and $\bar{\mathbf{A}}_s$ are given by

$$\mathbf{A} = \begin{Bmatrix} \alpha \\ \beta \\ \psi \end{Bmatrix}, \quad \bar{\mathbf{A}} = \begin{Bmatrix} \bar{\alpha} \\ \bar{\beta} \\ \bar{\psi} \end{Bmatrix}, \quad \bar{\mathbf{A}}_s = \begin{Bmatrix} \bar{\alpha}_s \\ \bar{\beta}_s \\ \bar{\psi}_s \end{Bmatrix}.$$

This leads to a static equation for the mean offset $\bar{\mathbf{A}}_s$ and the following equation of motion for the vessel:

$$[\mathbf{M}]\{\ddot{\mathbf{A}}\} + [\mathbf{C}]\{\dot{\mathbf{A}}\} + [\mathbf{K}][\{\mathbf{A}\} + \{\bar{\mathbf{A}}\}] + \gamma\{\mathscr{R}(\mathbf{A}, \bar{\mathbf{A}}, \bar{\mathbf{A}}_s)\} = \{\mathbf{F}\}, \tag{3}$$

where $[\mathbf{M}]$, $[\mathbf{C}]$ and $[\mathbf{K}]$ are the mass, damping and stiffness matrices of the vessel. The vector $\mathscr{R}(\mathbf{A}, \bar{\mathbf{A}}, \bar{\mathbf{A}}_s)$ denotes the nonlinear restoring forces arising due to nonlinearity of the mooring. It contains terms up to cubic in the vessel displacements for a multi-degree Duffing oscillator model. The strength of nonlinearity in the mooring stiffness is given by $\gamma$. The functional form of $\mathscr{R}(\mathbf{A}, \bar{\mathbf{A}}, \bar{\mathbf{A}}_s)$ depends on the mooring line arrangements, and is given in Section 4. It is assumed that the vessel is moored by identical mooring cables on either side. Consequently, a single parameter $\gamma$ is sufficient to describe the nonlinear mooring stiffness effect.

## 3. NONDIMENSIONAL EQUATIONS

The above set of equations is nondimensionalized with respect to wave amplitude $a$, acceleration due to gravity $g$ and wave number $k$, following Dean & Dalrymple (1993). The nondimensionalized variables are $\hat{\xi} = \xi/a$, $\hat{\psi} = \psi/ka$, $\hat{\varphi} = k\varphi/(a\sqrt{gk})$, $\hat{t} = \sqrt{gk}t$, $\hat{\mathbf{X}}' = k\mathbf{X}'$, $\delta = ka$ and $\varepsilon = \gamma a^2$. The nondimensional equations for $\varphi$ take the following form:

$$\hat{\varphi}_{\hat{t}\hat{t}} + \hat{\varphi}_{\hat{z}} = \delta[-2\nabla\hat{\varphi}\cdot\nabla\hat{\varphi}_{\hat{t}} + \hat{\varphi}_{\hat{t}}(\hat{\varphi}_{\hat{t}\hat{t}} + \hat{\varphi}_{\hat{z}})_{\hat{z}}] + \mathscr{O}(\delta^2) \quad \text{on } z = 0, \tag{4}$$

$$\begin{aligned} \mathbf{n}'\cdot\nabla\hat{\varphi} = \mathbf{n}'\cdot\{[\boldsymbol{\xi}_t + \hat{\boldsymbol{\Psi}}_t\times\hat{\mathbf{X}}'] + \delta\hat{\mathbf{H}}_t\hat{\mathbf{X}}' - \delta[(\hat{\boldsymbol{\xi}} + \hat{\boldsymbol{\Psi}}\times\hat{\mathbf{X}}')\cdot\nabla]\nabla\hat{\varphi}\} \\ + \delta(\hat{\boldsymbol{\Psi}}\times\mathbf{n})\cdot[(\hat{\boldsymbol{\xi}}_t + \hat{\boldsymbol{\Psi}}_t\times\hat{\mathbf{X}}') - \nabla\hat{\varphi}] + \mathscr{O}(\delta^3) \quad \text{on } S_m, \end{aligned} \tag{5}$$

and the nondimensional equations of motion are

$$\{\hat{\mathbf{A}}\}_{\hat{t}\hat{t}} + \frac{[\mathbf{M}]^{-1}[\mathbf{C}]}{\sqrt{gk}}\{\hat{\mathbf{A}}\}_{\hat{t}} + \frac{[\mathbf{M}]^{-1}[\mathbf{K}]}{gk}\{\hat{\mathbf{A}}\} + \varepsilon\frac{[\mathbf{M}]^{-1}\{\mathbf{R}\}}{gk} = \frac{[\mathbf{M}]^{-1}\{\mathbf{F}\}}{agk}. \tag{6}$$

The above set of equations forms a nonlinear boundary value problem with two independent small dimensionless parameters $\delta$ and $\varepsilon$. Consequently, we can express the nondimensional quantities in the following forms:

$$\hat{\varphi} = \hat{\varphi}_0^0 + \varepsilon\hat{\varphi}_1^0 + \delta\hat{\varphi}_0^1 + \delta\varepsilon\hat{\varphi}_1^1,$$

$$\hat{\mathbf{A}} = \hat{\mathbf{A}}_0^0 + \varepsilon\hat{\mathbf{A}}_1^0 + \delta\hat{\mathbf{A}}_0^1 + \delta\varepsilon\hat{\mathbf{A}}_1^1.$$

As our primary interest is in investigating the interactions of nonlinear mooring stiffness and wave hydrodynamics, we focus our attention on the higher-order perturbation term $\varepsilon\delta$ only, as this accounts for the aforementioned interaction effect. The terms proportional to $\varepsilon^2$ and $\delta^2$ are not considered here. This may be justified for the following reasons. As we are mainly interested in the resonant low-frequency response of the moored vessel, the hydrodynamic force proportional to $\delta^2$ is expected to have little contribution to the total response. Under the assumption of weak nonlinearity of the mooring stiffness, the perturbation term proportional to $\varepsilon^2$ may have insignificant effect on the total response of the structure. However, further studies are needed to justify these assumptions rigorously. On the other hand, the inclusion of the other higher-order terms would considerably increase the computational complexity of obtaining semi-analytical solutions for the wave hydrodynamics, even for a simple geometry of the vessel.

By equating the powers of $\delta$ and $\varepsilon$, a set of coupled linear differential equations is obtained which can be solved sequentially. The details of the procedure are described in Sarkar & Eatock Taylor (1998) for a single-degree-of-freedom system and will not be repeated here. It leads to the following equations involving the dynamic body boundary conditions on the undisturbed body surface $\bar{S}_m$, which are shown in dimensional form.

I. *Equations for* $(\delta^0, \varepsilon^0)$:

$$[\mathbf{M}]\{\ddot{\mathbf{A}}_0^0\} + [\mathbf{C}]\{\dot{\mathbf{A}}_0^0\} + [\mathbf{K}]\{\mathbf{A}_0^0\} = \{\mathbf{F}_0^0\}, \tag{7}$$

where

$$\{\mathbf{F}_0^0\} = \begin{Bmatrix} f_{0\alpha}^0 \\ f_{0\psi}^0 \\ f_{0\beta}^0 \end{Bmatrix}, \tag{8}$$

$$f_{0\alpha}^0 = -\rho \int_{\bar{S}_m} \varphi_{0t}^0 n_x \, \mathrm{d}s, \qquad f_{0\beta}^0 = -\rho \int_{\bar{S}_m} \varphi_{0t}^0 n_z \, \mathrm{d}s, \tag{9,10}$$

$$f_{0\psi}^0 = -\rho \int_{\bar{S}_m} \varphi_{0t}^0 (n_x z - n_z x) \, \mathrm{d}s. \tag{11}$$

II. *Equations for* $(\delta^0, \varepsilon^1)$:

$$[\mathbf{M}]\{\ddot{\mathbf{A}}_1^0\} + [\mathbf{C}]\{\dot{\mathbf{A}}_1^0\} + [\mathbf{K}]\{\mathbf{A}_1^0 + \overline{\mathbf{A}_1^0}\} = \{\mathbf{F}_1^0\}, \tag{12}$$

where

$$\{\mathbf{F}_1^0\} = \begin{Bmatrix} f_{1\alpha}^0 \\ f_{1\psi}^0 \\ f_{1\beta}^0 \end{Bmatrix} - \mathscr{R}(\mathbf{A}_0^0, \bar{\mathbf{A}}_s), \tag{13}$$

$$f_{1\alpha}^0 = -\rho \int_{\bar{S}_m} \varphi_{1t}^0 n_x \, \mathrm{d}s, \qquad f_{1\beta}^0 = -\rho \int_{\bar{S}_m} \varphi_{1t}^0 n_z \, \mathrm{d}s, \tag{14,15}$$

$$f_{1\psi}^0 = -\rho \int_{\bar{S}_m} \varphi_{1t}^0 (n_x z - n_z x) \, \mathrm{d}s. \tag{16}$$

III. *Equations for* $(\delta^1, \varepsilon^0)$:

$$[\mathbf{M}]\{\ddot{\mathbf{A}}_0^1\} + [\mathbf{C}]\{\dot{\mathbf{A}}_0^1\} + [\mathbf{K}]\{\mathbf{A}_0^1 + \overline{\mathbf{A}_0^1}\} = \{\mathbf{F}_0^1\}, \tag{17}$$

where

$$\{\mathbf{F}_0^1\} = \begin{Bmatrix} f_{0\alpha}^1 \\ f_{0\psi}^1 \\ f_{0\beta}^1 \end{Bmatrix}, \tag{18}$$

$$f_{0\alpha}^1 = -\rho \int_{\bar{S}_m} \{[\varphi_{0t}^1 + (\boldsymbol{\xi}_0^0 + \boldsymbol{\Psi}_0^0 \times \mathbf{X}) \cdot \nabla \varphi_{0t}^0 + \tfrac{1}{2} |\nabla \varphi_0^0|^2]\mathbf{n} + (\boldsymbol{\Psi}_0^0 \times \mathbf{n}) \varphi_{0t}^0\} \, \mathrm{d}s$$

$$+ \frac{\rho g}{2} \int_{\bar{C}_m} (\eta_0^0 - \beta_0^0 + x\psi_0^0)^2 \mathbf{n} \, \mathrm{d}l|_{\text{component along the } x\text{-axis}}, \tag{19}$$

$$f_{0\psi}^1 = -\rho \int_{\bar{S}_m} \{[\varphi_{0t}^1 + (\boldsymbol{\xi}_0^0 + \boldsymbol{\Psi}_0^0 \times \mathbf{X}) \cdot \nabla \varphi_{0t}^0 + \tfrac{1}{2} |\nabla \varphi_0^0|^2](\mathbf{X} \times \mathbf{n})$$

$$+ [(\boldsymbol{\xi}_0^0 \times \mathbf{n}) + (\boldsymbol{\Psi}_0^0 \times \mathbf{n}) \times \mathbf{X}] \varphi_{0t}^0\} \, \mathrm{d}s$$

$$+ \frac{\rho g}{2} \int_{\bar{C}_m} (\eta_0^0 - \beta_0^0 + x\psi_0^0)^2 (\mathbf{X} \times \mathbf{n}) \, \mathrm{d}l|_{\text{component along the } y\text{-axis}}, \tag{20}$$

where $\bar{C}_m$ is the contour defining the intersection of the undisturbed body with the undisturbed free surface.

IV. *Equations for* $(\delta^1, \varepsilon^1)$:

$$[\mathbf{M}]\{\ddot{\mathbf{A}}_1^1\} + [\mathbf{C}]\{\dot{\mathbf{A}}_1^1\} + [\mathbf{K}]\{\mathbf{A}_1^1 + \overline{\mathbf{A}_1^1}] = \{\mathbf{F}_1^1\}, \tag{21}$$

where

$$\{\mathbf{F}_1^1\} = \begin{Bmatrix} f_{1\alpha}^1 \\ f_{1\psi}^1 \\ f_{1\beta}^1 \end{Bmatrix} - \tilde{\mathbf{F}}(\mathbf{A}_0^0, \mathbf{A}_0^1, \bar{\mathbf{A}}_s), \tag{22}$$

$$f_{1\alpha}^1 = -\rho \int_{\bar{S}_m} \Bigg\{ \Bigg[ \varphi_{0t}^1 + \underbrace{(\boldsymbol{\xi}_0^0 + \boldsymbol{\Psi}_0^0 \times \mathbf{X}) \cdot \nabla \varphi_{1t}^0 + (\boldsymbol{\xi}_1^0 + \boldsymbol{\Psi}_1^0 \times \mathbf{X}) \cdot \nabla \varphi_{0t}^0}_{\text{I}}$$

$$+ \underbrace{\nabla \varphi_0^0 \cdot \nabla \varphi_1^0}_{\text{II}} \Bigg] \mathbf{n} + \underbrace{(\boldsymbol{\Psi}_0^0 \times \mathbf{n}) \varphi_{1t}^0 + (\boldsymbol{\Psi}_1^0 \times \mathbf{n}) \varphi_{0t}^0}_{\text{III}} \Bigg\} \mathrm{d}s$$

$$+ \rho g \int_{\bar{C}_m} \underbrace{(\eta_1^0 - \beta_1^0 + x\psi_1^0)(\eta_0^0 - \beta_0^0 + x\psi_0^0) \mathbf{n} \, \mathrm{d}l}_{\text{IV}} |_{\text{component along the } x\text{-axis}}, \tag{23}$$

$$f_{1\psi}^1 = -\rho \int_{\bar{S}_m} \Bigg\{ \Bigg[ \varphi_{0t}^1 + \underbrace{(\boldsymbol{\xi}_0^0 + \boldsymbol{\Psi}_0^0 \times \mathbf{X}) \cdot \nabla \varphi_{1t}^0 + (\boldsymbol{\xi}_1^0 + \boldsymbol{\Psi}_1^0 \times \mathbf{X}) \cdot \nabla \varphi_{0t}^0}_{\text{I}} + \underbrace{\nabla \varphi_0^0 \cdot \nabla \varphi_1^0}_{\text{II}} \Bigg] (\mathbf{X} \times \mathbf{n})$$

$$+ \underbrace{[(\boldsymbol{\xi}_0^0 \times \mathbf{n}) + (\boldsymbol{\Psi}_0^0 \times \mathbf{n}) \times \mathbf{X}] \varphi_{1t}^0 + [(\boldsymbol{\xi}_1^0 \times \mathbf{n}) + (\boldsymbol{\Psi}_1^0 \times \mathbf{n}) \times \mathbf{X}] \varphi_{0t}^0}_{\text{III}} \Bigg\} \mathrm{d}s$$

$$+ \rho g \int_{\bar{C}_m} \underbrace{(\eta_0^0 - \beta_0^0 + x\psi_0^0)(\eta_1^0 - \beta_1^0 + x\psi_1^0)(\mathbf{X} \times \mathbf{n}) \, \mathrm{d}l}_{\text{IV}} |_{\text{component along the } y\text{-axis}}. \tag{24}$$

Here $\tilde{\mathbf{F}}(\mathbf{A}_0^0, \mathbf{A}_0^1, \bar{\mathbf{A}}_s)$ denotes the perturbation term arising from the nonlinear restoring force directly, in the absence of fluid–structure interaction. The specific functional form of $\tilde{\mathbf{F}}$ depends on the nonlinear function $\mathscr{R}$ in equation (3).

## 4. ANALYSIS FOR A TRUNCATED CYLINDER

Based on the above formulation, a truncated cylinder shown in Figure 1 has been studied. The simple geometry of the vessel permits a semi-analytical solution. The solution of the first-order potential $\varphi_0^0$ is standard. It consists of two parts: the scattered potential $\varphi_s$, which consists of incident and diffracted potentials, and the radiation potential $\varphi_r$ which consists of three components, namely, surge potential $\varphi_\alpha$, heave potential $\varphi_\beta$, and pitch potential $\varphi_\psi$. The expression for the scattered potential of a wave with amplitude $a$ and frequency $\omega$ is given by (Huang & Eatock Taylor 1996)

$$\varphi_s = \begin{cases} \mathscr{R}e \sum_{n=0}^{\infty} \left[ \dfrac{\cosh\{k(z+h)\}}{\cosh(kh)} P_n(kr) + \sum_{j=0}^{\infty} B_{jn}^{\mathrm{Ex}} \dfrac{\mathrm{U}_n(m_j r)}{\mathrm{U}'_n(m_j R)} Z_j(m_j z) \right] \cos(n\theta) \mathrm{e}^{-\mathrm{i}\omega t} & (r \geq R, 0 \leq \theta \leq 2\pi), \\ \mathscr{R}e \sum_{n=0}^{\infty} \left[ \dfrac{1}{2} B_{0n}^{\mathrm{In}} \left( \dfrac{r}{R} \right) + \sum_{j=1}^{\infty} B_{jn}^{\mathrm{In}} \dfrac{\mathrm{I}_1(\lambda_n r)}{\mathrm{I}_1(\lambda_n R)} \cos(\lambda_j z) \right] \cos(n\theta) \mathrm{e}^{-\mathrm{i}\omega t} & (r \leq R, 0 \leq \theta \leq 2\pi), \end{cases} \tag{25}$$

where

$$P_n(kr) = -\frac{ga}{\omega} \varepsilon_n \mathrm{i}^{(n+1)} \left[ \mathrm{J}_n(kr) - \frac{\mathrm{J}'_n(kR)\mathrm{H}_n(kr)}{\mathrm{H}'_n(kR)} \right], \tag{26}$$

$$\mathrm{U}_n(m_j r) = \begin{cases} \mathrm{H}_n(m_0 r), & j = 0, \\ \mathrm{K}_n(m_j r), & j > 0, \end{cases} \tag{27}$$

$$Z_0 = \frac{1}{[\gamma_0(m_0)]^{1/2}} \cosh\{m_0(z+h)\}, \quad \gamma_0(m_0) = \frac{h}{2} \left[ 1 + \frac{\sinh(2m_0 h)}{2m_0 h} \right], \tag{28}$$

$$Z_j = \frac{1}{[\gamma_j(m_j)]^{1/2}} \cosh\{m_j(z+h)\}, \quad \gamma_j(m_j) = \frac{h}{2} \left[ 1 + \frac{\sinh(2m_j h)}{2m_j h} \right], \quad j > 0. \tag{29}$$

The term $\mathrm{H}_n(x)$ is the $n$th-order Hankel function of the first kind. $\varepsilon_0 = 1$; $\varepsilon_n = 2$, $n > 0$. $m_0 = k$ is the wavenumber of the incident wave, and $m_j, j > 0$ are the real roots of the equation

$$m_j \tan(m_j h) = -\frac{\omega^2}{g}. \tag{30}$$

The coefficients $B_{jn}^{\mathrm{Ex}}$ and $B_{jn}^{\mathrm{In}}$ are obtained from the boundary condition on the vertical surface of the cylinder, and by matching with the solution for the cylindrical column of fluid below the truncated cylinder. If the coefficients $B_{jn}^{\mathrm{Ex}}$ are set to zero, $\varphi_{0s}^0$ corresponds to the scattered potential of a bottom-seated vertical cylinder. The expression for the radiation potential is given by

$$\varphi_r = \mathscr{R}e\{\tilde{\alpha}_{0t}^0 \varphi_\alpha + \tilde{\beta}_{0t}^0 \varphi_\beta + \tilde{\psi}_{0t}^0 \varphi_\psi\}. \tag{31}$$

Here, $\tilde{\alpha}_{0t}^0$, $\tilde{\beta}_{0t}^0$ and $\tilde{\psi}_{0t}^0$ are the complex amplitudes of the first-order surge, heave and pitch motions.

Following Yeung (1981), the expressions for the radiation potentials can be written as

$$\varphi_\alpha = \begin{cases} \sum_{j=0}^{\infty} C_j^\alpha U_0(m_j r) Z_j(m_j z) \cos(\theta) e^{-i\omega t} & (r \geq R, 0 \leq \theta \leq 2\pi), \\ \left\{ \frac{1}{2} A_0^\alpha \left( \frac{r}{R} \right) + \sum_{j=1}^{\infty} A_j^\alpha \frac{I_1(\lambda_n r)}{I_1(\lambda_n R)} \cos(\lambda_j z) \right\} \cos(\theta) e^{-i\omega t} & (r \leq R, 0 \leq \theta \leq 2\pi), \end{cases} \tag{32}$$

$$\varphi_\beta = \begin{cases} \sum_{j=0}^{\infty} C_j^\beta U_0(m_j r) Z_j(m_j z) e^{-i\omega t} & (r \geq R, 0 \leq \theta \leq 2\pi), \\ \left\{ \frac{1}{2} A_0^\beta + \sum_{j=1}^{\infty} A_j^\beta \frac{I_0(\lambda_n r)}{I_0(\lambda_n R)} \cos(\lambda_j z) + \frac{1}{2d} \left( z^2 - \frac{r^2}{2} \right) \right\} e^{-i\omega t} & (r \leq R, 0 \leq \theta \leq 2\pi), \end{cases} \tag{33}$$

$$\varphi_\psi = \begin{cases} \sum_{j=0}^{\infty} C_j^\psi U_0(m_j r) Z_j(m_j z) \mathrm{Cos}(\theta) e^{-i\omega t} & (r \geq R, 0 \leq \theta \leq 2\pi), \\ \left\{ \frac{1}{2} A_0^\psi \left( \frac{r}{R} \right) + \sum_{j=1}^{\infty} A_j^\psi \frac{I_1(\lambda_n r)}{I_1(\lambda_n R)} \cos(\lambda_j z) - \frac{1}{2d} \left( z^2 r - \frac{r^3}{4} \right) \right\} \cos(\theta) e^{-i\omega t} & (r \leq R, 0 \leq \theta \leq 2\pi), \end{cases} \tag{34}$$

Using the perturbation expressions of the kinematic condition in the body boundary, it can be shown that $\varphi_1^0$ consists of only radiation potentials arising due to nonlinear body motions $\alpha_1^0$, $\beta_1^0$, $\psi_1^0$ and given by

$$\varphi_1^0 = \mathscr{R}e\{\tilde{\alpha}_{1t}^0 \varphi_\alpha + \tilde{\beta}_{1t}^0 \varphi_\beta + \tilde{\psi}_{1t}^0 \varphi_\psi\}, \tag{35}$$

where $\tilde{\alpha}_{1t}^0$, $\tilde{\beta}_{1t}^0$ and $\tilde{\psi}_{1t}^0$ are the complex amplitudes of surge, heave and pitch motion. In calculating the low-frequency forces, the effects of the nonlinear potentials $\varphi_0^1$ and $\varphi_1^1$ are neglected. This is analogous to the approximation usually made in calculating drift forces in random waves, and it permits analytical solutions to be obtained for the low frequency forces $\mathbf{F}_0^1$ and $\mathbf{F}_1^1$ with the already known potentials $\varphi_0^0$ and $\varphi_1^0$.

In the equation of motion, the mass and damping matrices of the floating structure (as shown in Figure 1) are

$$[\mathbf{M}] = \begin{bmatrix} m + m_{\alpha\alpha} & m_{\alpha\psi} & 0 \\ m_{\alpha\psi} & I + m_{\psi\psi} & 0 \\ 0 & 0 & m + m_{\beta\beta} \end{bmatrix}, \tag{36}$$

$$[\mathbf{C}] = \begin{bmatrix} c_{\alpha\alpha} & c_{\alpha\psi} & 0 \\ c_{\alpha\psi} & c_{\psi\psi} & 0 \\ 0 & 0 & c_{\beta\beta} \end{bmatrix}. \tag{37}$$

In the mass matrix $[\mathbf{M}]$, $m$ and $I$ are the mass and moment of inertia of the vessel in the dry state; $m_{\alpha\alpha}$, $m_{\psi\psi}$ and $m_{\beta\beta}$ indicate the added mass in surge, pitch and heave, respectively; and $m_{\alpha\psi}$ is the cross-added mass in surge and pitch. Similarly, $c_{\alpha\alpha}$, $c_{\psi\psi}$, $c_{\beta\beta}$ and $c_{\alpha\psi}$ are the damping for surge, pitch, heave and cross-added damping between surge and pitch, respectively. These damping terms are assumed to include the first-order added damping, mooring line damping, wave-drift and viscous damping.

Using a Duffing oscillator model, the nonlinear load–displacement characteristic of the cables on each side is given by

$$T = kx + \gamma k x^3, \tag{38}$$

where $T$, $x$, $k$ and $\gamma$ are the total axial tension of the cables, axial cable displacement due to vessel motion, total linear cable stiffness, and strength of nonlinearity in the cable stiffness, respectively. The stiffness matrix for the specified mooring arrangement is then

$$[\mathbf{K}] = \begin{bmatrix} k_{\alpha\alpha} & k_{\alpha\psi} & 0 \\ k_{\alpha\psi} & k_{\psi\psi} & 0 \\ 0 & 0 & k_{\beta\beta} \end{bmatrix}, \tag{39}$$

where $k_{\alpha\alpha} = 2k\cos^2\theta$; $k_{\alpha\psi} = 2k\cos\theta(b\cos\theta + R\sin\theta)$; $k_{\psi\alpha} = k_{\alpha\psi}$; $k_{\psi\psi} = 2k(b\cos\theta + R\sin\theta)^2 + W \times GM$ and $k_{\beta\beta} = 2k\sin^2\theta + \rho\pi R^2 g$. $W$, $GM$ and $\theta$ are the weight, metacentric height and cable inclination to the horizontal, and $b$ is the height of the point of attachment of the cables above the base of the cylinder. Consequently, the vector $\{\mathscr{R}\}$ in equation (3), representing the nonlinearity of the mooring restoring force for the configuration in Figure 1, is given by

$$\{\mathscr{R}\} = \begin{Bmatrix} k[(\chi_l + \mu)^3 + (\chi_r + \mu)^3 - 2\mu^3] \\ k(R\sin\theta + b\cos\theta)[(\chi_l + \mu)^3 + (\chi_r + \mu)^3 - 2\mu^3] \\ k[(\chi_l + \mu)^3 - (\chi_r + \mu)^3] \end{Bmatrix}, \tag{40}$$

where $\chi_l = [(\alpha + b\psi)\cos\theta + (\beta + R\psi)\sin\theta]$, $\chi_r = [(\alpha + b\psi)\cos\theta - (\beta - R\psi)\sin\theta]$, $l$ and $r$ designating left- and right-side mooring lines; $\mu = \bar{\alpha}_s\cos\theta$ and $\bar{\alpha}_s$ = surge offset due to wind and current. For simplicity, the effects of mean pitch angle $\bar{\psi}_s$ and heave displacement $\bar{\beta}_s$ due to wind and current are assumed to be negligible compared with $\bar{\alpha}_s$ in the nonlinear restoring vector $\mathscr{R}$. However, this assumption can easily be relaxed, which will result in more complex algebraic expressions for the elements of the nonlinear restoring vector $\mathscr{R}$. It can be noted that although the mooring force is approximated by a cubic polynomial in the displacements, a quadratic component also arises in the dynamic equations of the vessel, arising from the offset due to wind/current. It is also worth noting that the surge, heave and pitch motions are coupled through nonlinearity in the mooring stiffness. In the case of a linear mooring, the surge and pitch motions are uncoupled from the heave motion.

## 5. POWER SPECTRAL DENSITY OF FORCE AND RESPONSE

In this section, power spectral densities of the forces and responses are obtained corresponding to input by a two-sided wave elevation spectrum $G_\eta(\omega)$. The representation of the first-order force spectra is routine and given by

$$[\mathbf{G}_{f_0^0}(\omega)] = [\mathscr{F}(\omega)][\bar{\mathscr{F}}(\omega)]G_\eta(\omega), \tag{41}$$

where the overbar denotes complex conjugate. The term $[\mathscr{F}(\omega)]$ is the first-order force-transfer function matrix which represents the surge, pitch and heave exciting forces due to a unit amplitude harmonic wave with frequency $\omega$. The expressions for the first-order surge, pitch and heave exciting force transfer functions are known (Garrett 1971) and will not be discussed here. The first-order power spectral density matrix of the response is then given by

$$[\mathbf{G}_{A_0^0}(\omega)] = [\mathscr{H}(\omega)][\mathbf{G}_{f_0^0}(\omega)][\bar{\mathscr{H}}(\omega)], \tag{42}$$

where $[\mathscr{H}(\omega)]$ is the frequency response matrix corresponding to the vessel dynamic displacements.

The power spectral density matrix (PSD) of $\mathscr{R}(\mathbf{A}_0^0, \bar{\mathbf{A}}_s)$ is now determined. The first step is to obtain the power spectral densities for $(\chi_l + \mu)$ and $(\chi_r + \mu)$. Using the Volterra series

technique (Schetzen 1979), it can be shown that (neglecting the spike at $\omega = 0$ due to mean response components arising from the nonlinearities) a typical spectrum is

$$G_{(\chi_l+\mu)^3}(\omega) = 6\int_{-\infty}^{\infty}\int_{-\infty}^{\infty} G_{\chi_l\chi_l}(\omega-\omega_1)G_{\chi_l\chi_l}(\omega_2)G_{\chi_l\chi_l}(\omega_2-\omega_1)\,\mathrm{d}\omega_1\,\mathrm{d}\omega_2$$
$$+ 2(3\mu)^2\int_{-\infty}^{\infty} G_{\chi_l\chi_l}(\omega_1)G_{\chi_l\chi_l}(\omega-\omega_1)\,\mathrm{d}\omega_1$$
$$+ (3\mu^2)^2 G_{\chi_l\chi_l}(\omega) + 6(3\mu^2)\sigma^2 \times G_{\chi_l\chi_l}(\omega). \tag{43}$$

Here, $\sigma^2$ is the variance of $\chi_l$. The expressions for the two-sided spectra $G_{(\chi_r+\mu)^3}(\omega)$ and $G_{(\chi_l+\mu)^3(\chi_r+\mu)^3}(\omega)$ can be obtained from equation (43) just by replacing $\chi_l\chi_l$ by $\chi_r\chi_r$, and $\chi_l\chi_r$, respectively. The above expressions enable one to determine the PSD matrix $[\mathbf{G}_{\mathscr{R}}(\omega)]$ of $\mathscr{R}(\mathbf{A}_0^0, \bar{\mathbf{A}}_s)$ in a straightforward manner. Then the PSD matrix of $\mathbf{A}_1^0$ is given by

$$[\mathbf{G}_{A_1^0}(\omega)] = [\mathscr{H}(\omega)][\mathbf{G}_{\mathscr{R}}(\omega)][\bar{\mathscr{H}}(\omega)]. \tag{44}$$

The next step is to determine the spectrum of low-frequency second-order forces. In analysing the second-order responses, only surge and pitch degrees of freedom are considered [which are uncoupled from heave motion in the perturbation equations (7), (12), (17) and (21)]. Using a two-term Volterra series expansion, the one-sided power spectral densities of the low-frequency second-order forces can be written as (Langley 1987)

$$S_{f_{0\alpha}^1}(\omega) = 8\int_0^{\infty} |\Gamma_{0\alpha}^1(\omega_1, \omega+\omega_1)|^2 S_\eta(\omega_1)S_\eta(\omega+\omega_1)\,\mathrm{d}\omega_1, \tag{45}$$

$$S_{f_{0\psi}^1}(\omega) = 8\int_0^{\infty} |\Gamma_{0\psi}^1(\omega_1, \omega+\omega_1)|^2 S_\eta(\omega_1)S_\eta(\omega+\omega_1)\,\mathrm{d}\omega_1, \tag{46}$$

$$S_{f_{0\alpha}^1 f_{0\psi}^1}(\omega) = 8\int_0^{\infty} \Gamma_{0\alpha}^1(\omega_1, \omega+\omega_1)\bar{\Gamma}_{0\psi}^1(\omega_1, \omega+\omega_1)S_\eta(\omega_1)S_\eta(\omega+\omega_1)\,\mathrm{d}\omega_1, \tag{47}$$

where $\Gamma_{0\alpha}^1$ and $\Gamma_{0\psi}^1$ are the conventional second-order force transfer functions defined by the forces on the vessel due to two unit amplitude waves in bi-harmonic seas (Eatock Taylor & Huang 1997).

From equations (23) and (24), it can be shown that the forces $f_{1\alpha}^1$ and $f_{1\psi}^1$ can be written as

$$f_{1\alpha}^1 = \Gamma_{1\alpha\alpha}^1(\omega_1, \omega_2)a\tilde{\alpha}_1^0 + \Gamma_{1\alpha\psi}^1(\omega_1, \omega_2)a\tilde{\psi}_1^0 + \Gamma_{1\alpha\beta}^1(\omega_1, \omega_2)a\tilde{\beta}_1^0, \tag{48}$$

$$f_{1\psi}^1 = \Gamma_{1\psi\alpha}^1(\omega_1, \omega_2)a\tilde{\alpha}_1^0 + \Gamma_{1\psi\psi}^1(\omega_1, \omega_2)a\tilde{\psi}_1^0 + \Gamma_{1\psi\beta}^1(\omega_1, \omega_2)a\tilde{\beta}_1^0. \tag{49}$$

The terms $\Gamma_{1\alpha\alpha}^1(\omega_1, \omega_2)$, $\Gamma_{1\alpha\psi}^1(\omega_1, \omega_2)$ and $\Gamma_{1\alpha\beta}^1(\omega_1, \omega_2)$ are the new nonlinear force transfer functions (symmetric in frequency) defined as the low-frequency hydrodynamic surge force when a unit amplitude wave at one frequency interacts with a unit amplitude surge, pitch and heave motion at a second frequency, respectively. Similar definitions can be introduced for the terms $\Gamma_{1\psi\alpha}^1$, $\Gamma_{1\psi\psi}^1$ and $\Gamma_{1\psi\beta}^1$ representing nonlinear pitch force transfer functions. The expressions for the low-frequency one-sided force spectra $S_{f_{1\alpha}^1}$, $S_{f_{1\psi}^1}$ and $S_{f_{1\alpha}^1 f_{1\psi}^1}$ have been derived. As these expressions involve complicated convolutions, only a typical expression, namely $S_{f_{1\alpha}^1}$ is given here:

$$S_{f_{1\alpha}^1}(\omega) = 2\int_0^{\infty} [|\Gamma_{1\alpha\alpha}^1(\omega_1, \omega+\omega_1)|^2 \{S_{\alpha_1^0}(\omega_1)S_\eta(\omega+\omega_1) + S_{\alpha_1^0}(\omega+\omega_1)S_\eta(\omega_1)$$
$$+ \mathscr{R}e[S_{\eta\alpha_1^0}(-\omega_1)S_{\alpha_1^0\eta}(\omega+\omega_1) + S_{\eta\alpha_1^0}(\omega+\omega_1)S_{\alpha_1^0\eta}(-\omega_1)]\}$$

$$+ |\Gamma^1_{1\alpha\psi}(\omega_1, \omega + \omega_1)|^2 \{S_{\psi_1^0}(\omega_1) S_\eta(\omega + \omega_1) + S_{\psi_1^0}(\omega + \omega_1) S_\eta(\omega_1)$$

$$+ \mathscr{R}e[S_{\eta\psi_1^0}(\omega_1) S_{\psi_1^0\eta}(\omega + \omega_1) + S_{\eta\psi_1^0}(\omega + \omega_1) S_{\psi_1^0\eta}(\omega_1)]\}$$

$$+ 2\mathscr{R}e[\Gamma^1_{1\alpha\alpha}(\omega_1, \omega + \omega_1) \bar{\Gamma}^1_{1\alpha\psi}(\omega_1, \omega + \omega_1) \{S_{\alpha_1^0\psi_1^0}(\omega_1) S_\eta(\omega + \omega_1)$$

$$+ S_{\alpha_1^0\psi_1^0}(\omega + \omega_1) S_\eta(\omega_1) + S_{\eta\psi_1^0}(\omega_1) S_{\alpha_1^0\eta}(\omega + \omega_1) + S_{\eta\psi_1^0}(\omega + \omega_1) S_{\alpha_1^0\eta}(\omega_1)\}]$$

$$+ |\Gamma^1_{1\alpha\beta}(\omega_1, \omega + \omega_1)|^2 \{S_{\beta_1^0}(\omega_1) S_\eta(\omega + \omega_1) + S_{\beta_1^0}(\omega + \omega_1) S_\eta(\omega_1)$$

$$+ \mathscr{R}e[S_{\eta\beta_1^0}(-\omega_1) S_{\beta_1^0\eta}(\omega + \omega_1) + S_{\eta\beta_1^0}(\omega + \omega_1) S_{\beta_1^0\eta}(-\omega_1)]\}] \, \mathrm{d}\omega_1. \tag{50}$$

The expressions for $S_{f^1_{1\psi}}$ and $S_{f^1_{1\alpha} f^1_{1\psi}}$ are given in Appendix A. The power spectral density matrix for the nonlinear forces derived above can be used to determine the low-frequency second-order responses in a straightforward manner.

## 6. NUMERICAL RESULTS

As an example of the above formulation, results have been obtained for a truncated cylinder with radius $R = 10$ m, draught $d = 30$ m floating in water depth $h = 100$ m. From the available first-order potentials, the expressions for the second-order forces $f^1_{0\alpha}$ and $f^1_{0\psi}$ have been derived. To simplify the analysis, the scattered potential due to the truncated cylinder can be approximated by that of a bottom-seated cylinder (Huang & Eatock Taylor 1996; Sarkar & Eatock Taylor 1998) in calculating all the second-order forces. The validity of this approximation, which significantly simplifies the derivation of analytical expressions for the various terms, has been justified for the truncated cylinder by comparing results with those obtained using a numerical approach. This was shown in Sarkar & Eatock Taylor (1998) in relation to the surge drift force. It should be emphasized, however, that no such approximation is made while calculating the radiation potentials and the first-order forces.

Both $f^1_{0\alpha}$ and $f^1_{0\psi}$ can be divided into two parts: one when the body is assumed to be fixed, and the other due to first-order body motion. Furthermore, the second part consists of three components, which are linearly proportional to first-order surge, heave and pitch motions. Figure 2 illustrates the effect of first-order body motions on the mean second-order surge force and pitch moment. To achieve clarity in this particular figure, the hydrostatic stiffnesses are here neglected in calculating the first-order body motion, to avoid the rapid variations in the mean drift force and pitch moment near the heave and pitch resonances. It is quite evident that both surge and pitch motion can significantly influence the mean force and moment, $f^1_{0\alpha}$ and $f^1_{0\psi}$. The effect of first-order heave motion on $f^1_{0\alpha}$ and $f^1_{0\psi}$ is negligible in this specific case, and is not shown in the figure.

Figure 3 shows the new nonlinear transfer functions $\Gamma^1_{1\alpha\alpha}(\omega_1, \omega_2)$, $\Gamma^1_{1\alpha\psi}(\omega_1, \omega_2)$, $\Gamma^1_{1\psi\alpha}(\omega_1, \omega_2)$, $\Gamma^1_{1\psi\psi}(\omega_1, \omega_2)$, $\Gamma^1_{1\alpha\beta}(\omega_1, \omega_2)$ and $\Gamma^1_{1\psi\beta}(\omega_1, \omega_2)$ at $\omega_1 = \omega_2 = \omega$. From equations (23) and (24), each of these transfer functions consists of components from terms (I), (II), (III) and (IV). The contributions of all these terms to each of these transfer functions are also plotted in Figure 3. It can be seen that $\Gamma^1_{1\alpha\psi}(\omega, \omega)$ and $\Gamma^1_{1\psi\alpha}(\omega, \omega)$ satisfy the expected reciprocity requirement, to a good approximation. The slight error in reciprocity may be due to the approximations in the first-order diffraction potentials used in the various expressions. Physically, the term $\Gamma^1_{1\alpha\psi}(\omega, \omega)$ can be interpreted as the mean surge force arising due to the interaction of a unit amplitude wave and a unit amplitude pitch motion at frequency $\omega$. Similarly, $\Gamma^1_{1\psi\alpha}(\omega, \omega)$ is the mean pitch moment arising due to interaction of a unit amplitude wave and a unit amplitude surge motion at frequency $\omega$. The simpler expressions for $\Gamma^1_{1\alpha\psi}(\omega, \omega)$ and $\Gamma^1_{1\psi\alpha}(\omega, \omega)$ are given for a bottom-mounted cylinder in Appendix B. These expressions have been used to check the program for the solution of

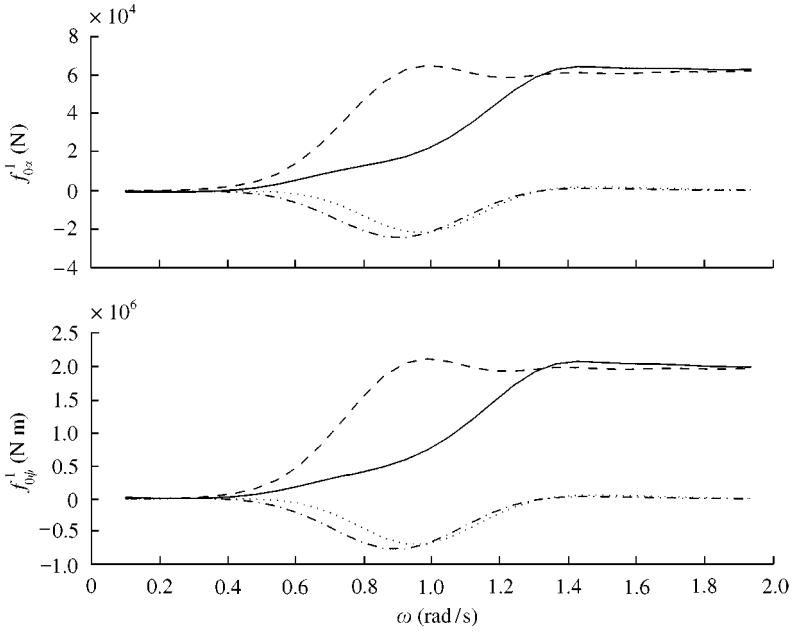


Figure 2. Variation of mean force/moment with frequency: – – –, fixed body; ——, moving body; –·–·–, surge contribution; ·····, pitch contribution.

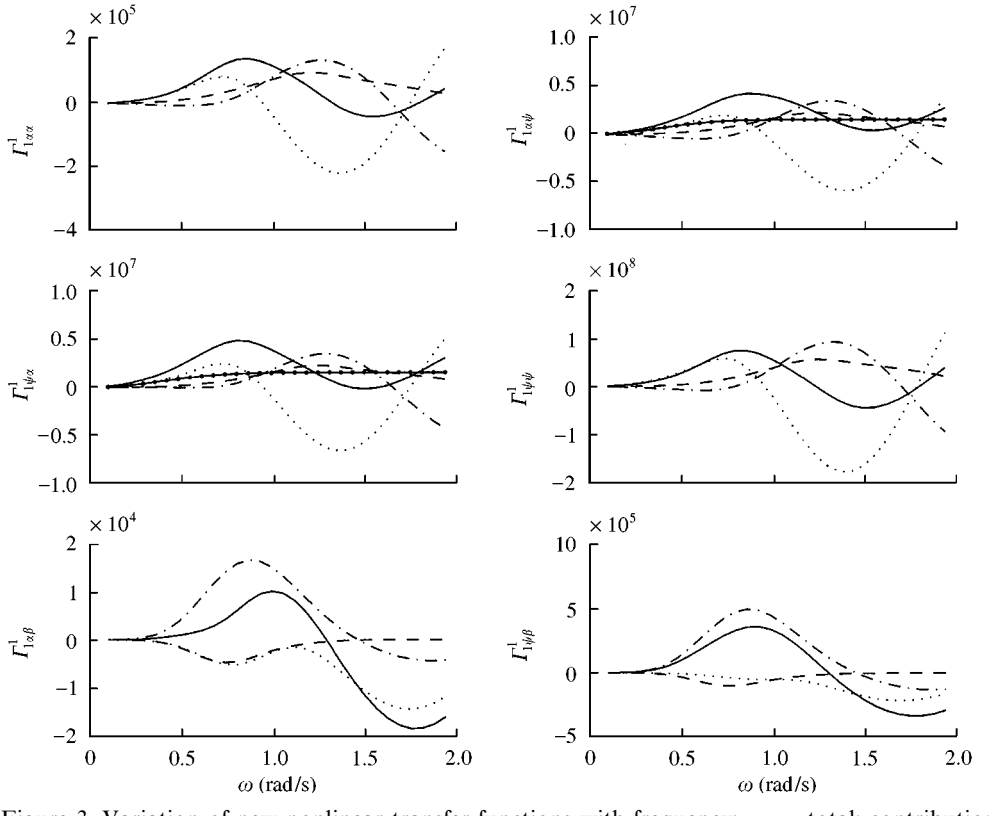


Figure 3. Variation of new nonlinear transfer functions with frequency: ——, total; contribution from: (I) — — —; (II) –·–·–; (III) –•–•–; and (IV) ·····.

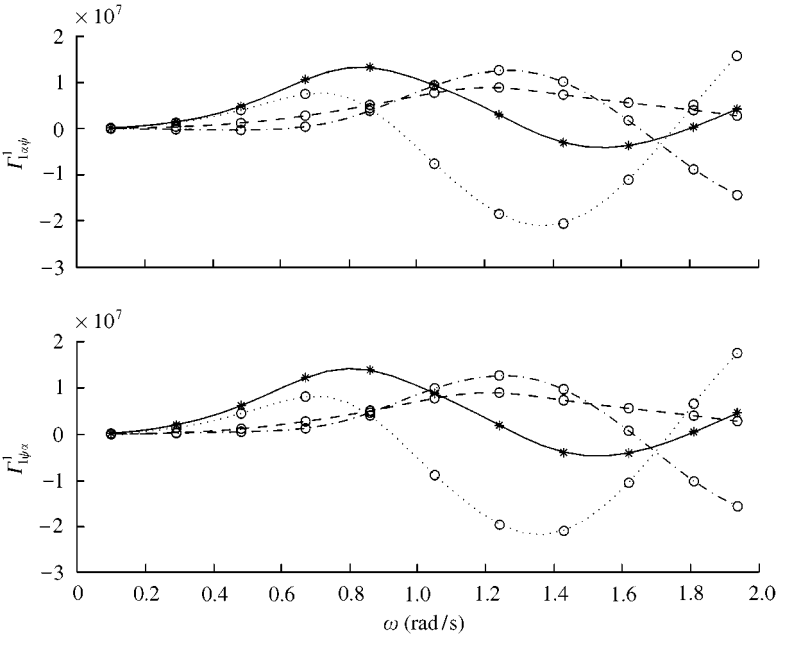


Figure 4. Validation with bottom-seated cylinder: ——, total for truncated cylinder; ∗−∗−∗, total for bottom-seated cylinder; contribution from: (I) — — —; (II) –·–·–; (IV) ····· for truncated cylinder, and ◦◦◦ for bottom-seated cylinder.

the truncated cylinder in the limiting case when the truncation depth goes to zero. Figure 4 shows the comparison of the results in the two cases: the semi-analytical solution derived for a truncated cylinder and a bottom-seated cylinder.

Next, the power spectral densities of the forces and responses are considered for various system parameters. In calculating the response of the vessel, the linear mooring stiffness $k$ is taken to be $5.5 \times 10^5$ N/m. The density of the vessel is three quarters the density of water and the metacentric height $GM$ is 2.5 m. The choice of damping is somewhat arbitrary in order to simplify the interpretation. In any case, there remains considerable uncertainty about appropriate values to use for damping of the nonlinear responses of realistic configurations. The total damping values in low-frequency first- and second-order motions are here taken to be five times and 15 times the first-order radiation damping. The mean offset $\bar{\alpha}_s$ due to wind/current is taken to be zero. The one-sided power spectral density $S_\eta$ of the wave elevation corresponds to the ISSC spectrum [e.g., Bishop & Price (1979)] with significant wave height $H_s = 13.5$ m and mean zero crossing period $T_z = 9.5$ s. Different systems are considered by varying the cable connection points ($b$ in Figure 1) and nonlinear mooring stiffness parameter $\gamma$. Three cases are considered: $b = 0.35d$, $\gamma = 0.1$ (case A); $b = 0.4d$, $\gamma = 0.07$ (case B); and $b = 0.45d$, $\gamma = 0.016$ (case C).

Figure 5 shows the frequency response functions $\mathscr{H}(\omega)$ of the vessel for surge and pitch motions for various cases. In can be observed that the increasing distance to the cable connection points ($b$) steadily increases the distance between the two resonance frequencies, as observed from the transfer functions for the surge and pitch. The low and high fundamental frequencies correspond to predominantly surge and pitch modes, respectively, for the three cases considered. Furthermore, it can also be observed that the cable connection points do not influence the anti-resonance point in the pitch transfer functions. It is also worth mentioning that the heave motion is uncoupled from the surge and pitch motions for the specific mooring arrangements considered here.

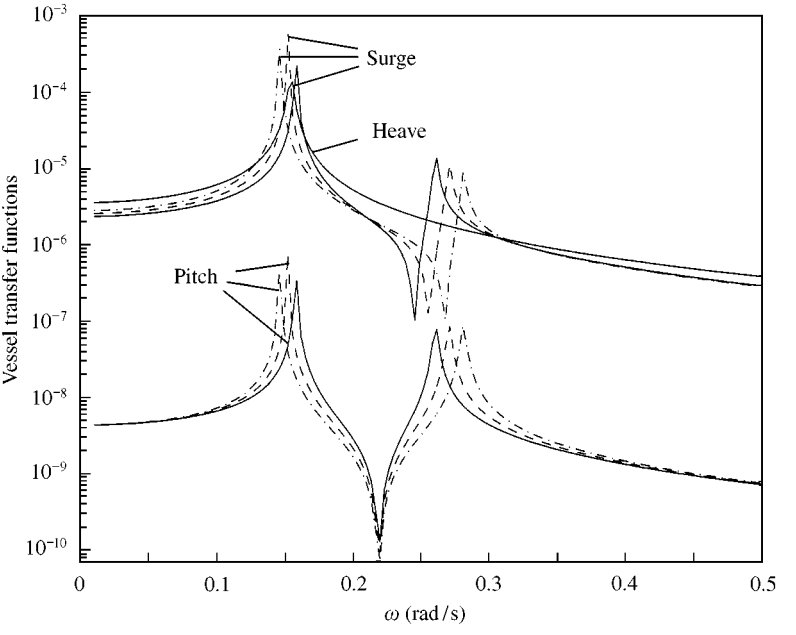


Figure 5. Frequency response functions of the vessel: ——, Case A; – – –, Case B; –·–·–, Case C.

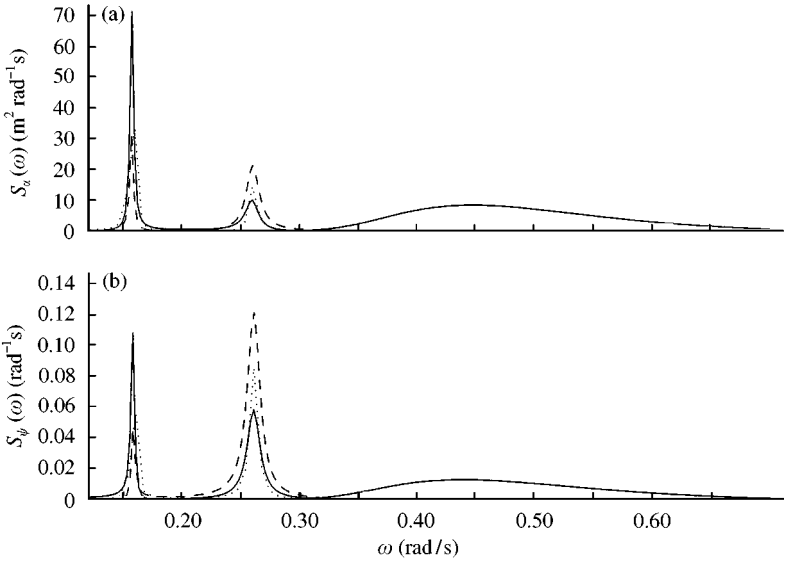


Figure 6. Case A: autospectral densities of response: —, $f_0^0$; —, $f_0^1$; – – –, $f_1^1$; ·····, $f_1^0$.

Figure 6 shows the auto-spectral densities of the low-frequency nonlinear responses for case A. As mentioned before, the new nonlinear forces $f_{1\alpha}^1$ and $f_{1\psi}^1$ arise because of the interaction of the incoming wave with the low-frequency first-order resonant responses $\alpha_1^0$, $\beta_1^0$ and $\psi_1^0$. For this specific case, it seems that there is a significant contribution from the first order nonlinear pitch motion $\psi_1^0$; this can effectively give rise to low (difference) frequency forces as a result of the convolution, because the predominant pitch

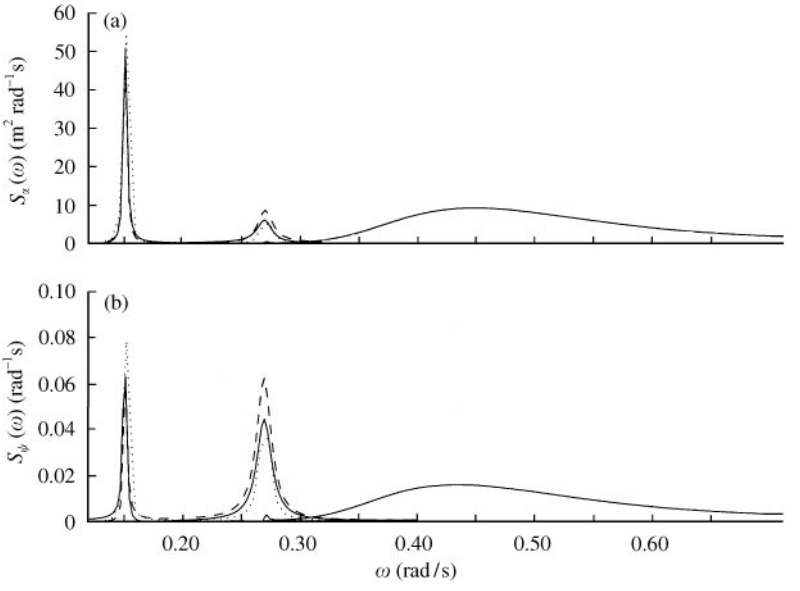


Figure 7. Case B: autospectral densities of response: —, $f_0^0$; —, $f_0^1$; – – –, $f_1^1$; · · · · ·, $f_1^0$.

resonance frequency is closer to the peak of the wave spectrum than the predominant surge resonant frequency. In general, $\alpha_1^0$, $\beta_1^0$ and $\psi_1^0$ can all contribute to $f_{1\alpha}^1$ and $f_{1\psi}^1$ depending on the system parameters. The effect of $\beta_1^0$ on $f_{1\alpha}^1$ and $f_{1\psi}^1$ is negligible for the three cases studied here. In this calculatiion of the nonlinear responses $\alpha_1^1$ and $\psi_1^1$, the effect of the last term in equation (22), namely $\tilde{\mathbf{F}}(\mathbf{A}_0^0, \mathbf{A}_1^0, \bar{\mathbf{A}}_s)$, was omitted in the interest of brevity, but it should be noted that this can also contribute to the total response, as indicated in Sarkar & Eatock Taylor (1998).

Figure 7 shows the spectra of responses for case B. In this case, the predominant pitch resonance frequency falls just within the band-width of the wave spectrum, as observed from the presence of the minute resonant peaks in the first-order wave frequency surge ($\alpha_0^0$) and pitch ($\psi_0^0$) responses. In this case, both nonlinear surge ($\alpha_1^0$) and pitch ($\psi_1^0$) responses are significant, and a comparatively weak nonlinearity in the mooring can produce significant nonlinear surge and pitch responses, namely, $\alpha_1^1$ and $\psi_1^1$.

The spectra of responses for case C are shown in Figure 8. In this case, the first-order pitch response is strongly influenced by the resonance effects. However, the first-order nonlinear surge ($\alpha_1^0$) and pitch ($\psi_1^0$) responses are now dominated by the predominant surge mode, as observed from the locations of the peaks in the spectra of $\alpha_1^0$ and pitch $\psi_1^0$. Furthermore, it can be noticed that the contributions of first-order nonlinear responses $\alpha_1^0$ and $\psi_1^0$ now exceed the contributions due to $\alpha_1^1$ and $\psi_1^1$, the response arising due to nonlinear wave–structure interactions.

## 7. CONCLUDING REMARKS

A method developed to determine the low-frequency surge wave forces on a nonlinearly moored vessel has been extended to consider the multi-degree rigid-body dynamics of a floating structure. The nonlinear dynamic behavior of the structure is modelled as a Duffing oscillator undergoing surge, heave and pitch motions. Under the assumption of small wave slope and weak nonlinearity of the mooring stiffness, a two-scale perturbation

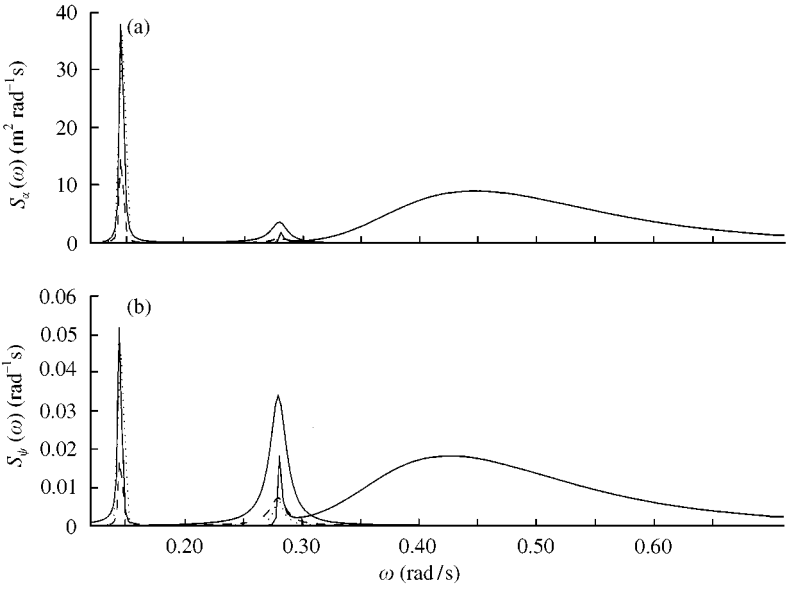


Figure 8. Case C: autospectral densities of response: —, $f_0^0$; —, $f_0^1$; – – –, $f_1^1$; · · · · ·, $f_1^0$.

technique has been extended to solve the nonlinear water-wave boundary value problem. As an example of the formulation, a semi-analytical solution has been derived for a floating truncated cylinder in finite water depth. It is found that the additional low frequency first-order responses arising due to nonlinear mooring stiffness interact with the incoming wave to give rise to additional low-frequency forces. These additional new low-frequency forces are solely due to the nonlinear mooring stiffness. The magnitudes of these new forces can be comparable to those of conventional second-order forces calculated without taking into account the nonlinear dynamics of the vessel.

From a statistical point of view, the conventional second-order forces arising in a linearly moored vessel are the second-order transformation of a Gaussian random process. On the other hand, the new nonlinear forces arising in a nonlinearly moored vessel are the polynomials (up to fourth degree for a Duffing's oscillator model) of a Gaussian random process. These strongly non-Gaussian forces give rise to tuned resonant responses which could significantly influence the statistics of the extreme responses of the floating vessel.

The results reported in this paper are based on the simplest form of an axisymmetric floating body, namely a truncated cylinder. Extending this analysis to the more general case of multi-column offshore platforms such as a semi-submersible, considering the six-degree-of-freedom rigid-body dynamics of the vessel and effects of spread seas, will certainly shed more light on the understanding of complex nonlinear wave–structure interactions addressed here. Furthermore, the results are based on a somewhat arbitrary choice of the damping coefficients, both to simplify the analysis and to highlight the effects of the nonlinear interaction of the mooring stiffness and the wave hydrodynamics. Further investigation is necessary to resolve these issues.

## ACKNOWLEDGEMENTS

The first author gratefully acknowledges the financial support of a Felix Scholarship granted by the Felix Trust through Oxford University.

## References


Bishop, R. E. D. & Price, W. G. 1979 *Hydroelasticity of Ships*. Camridge: Cambridge University Press.

Dean, R. G. & Dalrymple, R. A. 1993 *Water Wave Mechanics for Engineers and Scientists*. Singapore: World Scientific Press.

Drake, K. R., Eatock Taylor, R. & Matsui, T. 1984 Drift of an articulated cylinder in regular waves. *Proceedings of the Royal Society of London* A **394,** 363–385.

Eatock Taylor, R. & Huang, J. B. 1997 Semi-analytical formulation for second order diffraction by a vertical cylinder in bichromatic waves. *Journal of Fluids and Structures* **11,** 465–484.

Garrett, C. J. R. 1971 Wave forces on a circular dock. *Journal of Fluid Mechanics* **46,** 129–139.

Huang, J. B. & Eatock Taylor, R. 1996 Semi-analytical solution for second-order wave diffraction by a truncated circular cylinder in monochromatic waves. *Journal of Fluid Mechanics* **319,** 171–196.

Langley, R. S. 1987 Second order frequency domain analysis of moored vessels. *Applied Ocean Research* **9,** 7–17.

MacCamy, R. C. & Fuchs, R. A. 1954 Wave forces on piles: a diffraction theory. U.S. Army Coastal Engineering Center, Tech. Mem., no. 69.

Ogilvie, T. F. 1983 Second-order hydrodynamic effects on ocean platforms. *Proceedings of International Workshop on Ship and Platform Motions,* Berkeley, CA, U.S.A., pp. 205–265.

Petrauskas, C. 1976 Hydrodynamic damping and added mass for flexible offshore platforms. Ph. D. Thesis, University of California, Berkeley, CA, U.S.A.

Schetzen, M. 1979 *The Volterra and Wiener Theories of Nonlinear Systems* New York: John Wiley & Sons.

Sarkar, A. & Eatock Taylor, R. 1998 Low frequency responses of non-linearly moored vessels in random waves: development of a two scale perturbation method. *Applied Ocean Research* **4,** 225–236.

Yeung, R. W. 1981 Added mass and damping of a vertical cylinder in finite-depth waters. *Applied Ocean Research* **3,** 119–133.


## APPENDIX A: POWER SPECTRAL DENSITIES OF NEW NONLINEAR FORCES

The expressions for $S_{f^1_{1\psi}}$ and $S_{f^1_{1\alpha}f^1_{1\psi}}$, analogous to $S_{f^1_{1\alpha}}$ in equation (50), are the following:

$$
\begin{aligned}
S_{f^1_{1\psi}}(\omega) = 2\int_0^\infty \big[ & |\Gamma^1_{1\psi\alpha}(\omega_1, \omega+\omega_1)|^2 \{S_{\alpha_1^o}(\omega_1)S_\eta(\omega+\omega_1) + S_{\alpha_1^o}(\omega+\omega_1)S_\eta(\omega_1) \\
& + \mathscr{R}e[S_{\eta\alpha_1^o}(-\omega_1)S_{\alpha_1^o\eta}(\omega+\omega_1) + S_{\eta\alpha_1^o}(\omega+\omega_1)S_{\alpha_1^o\eta}(-\omega_1)]\} \\
& + |\Gamma^1_{1\psi\psi}(\omega_1, \omega+\omega_1)|^2 \{S_{\psi_1^o}(\omega_1)S_\eta(\omega+\omega_1) + S_{\psi_1^o}(\omega+\omega_1)S_\eta(\omega_1) \\
& + \mathscr{R}e[S_{\eta\psi_1^o}(\omega_1)S_{\psi_1^o\eta}(\omega+\omega_1) + S_{\eta\psi_1^o}(\omega+\omega_1)S_{\psi_1^o\eta}(\omega_1)]\} \\
& + 2\,\mathscr{R}e\{\Gamma^1_{1\psi\alpha}(\omega_1, \omega+\omega_1)\bar{\Gamma}^1_{1\psi\psi}(\omega_1, \omega+\omega_1)[S_{\alpha_1^o\psi_1^o}(\omega_1)S_\eta(\omega+\omega_1) \\
& + S_{\alpha_1^o\psi_1^o}(\omega+\omega_1)S_\eta(\omega_1) + S_{\eta\psi_1^o}(\omega_1)S_{\alpha_1^o\eta}(\omega+\omega_1) + S_{\eta\psi_1^o}(\omega+\omega_1)S_{\alpha_1^o\eta}(\omega_1)]\} \\
& + |\Gamma^1_{1\psi\beta}(\omega_1, \omega+\omega_1)|^2 \{S_{\beta_1^o}(\omega_1)S_\eta(\omega+\omega_1) + S_{\beta_1^o}(\omega+\omega_1)S_\eta(\omega_1) \\
& + \mathscr{R}e[S_{\eta\beta_1^o}(-\omega_1)S_{\beta_1^o\eta}(\omega+\omega_1) + S_{\eta\beta_1^o}(\omega+\omega_1)S_{\beta_1^o\eta}(-\omega_1)]\}\big]\,\mathrm{d}\omega_1, \qquad \text{(A1)}
\end{aligned}
$$

$$
\begin{aligned}
S_{f^1_{1\alpha}f^1_{1\psi}}(\omega) = 2\int_0^\infty \big[ & \Gamma^1_{1\alpha\alpha}(\omega_1, \omega+\omega_1)\bar{\Gamma}^1_{1\alpha\psi}(\omega_1, \omega+\omega_1)\{S_{\alpha_1^o}(\omega_1)S_\eta(\omega+\omega_1) \\
& + S_{\alpha_1^o}(\omega+\omega_1)S_\eta(\omega_1) + S_{\eta\alpha_1^o}(-\omega_1)S_{\alpha_1^o\eta}(\omega+\omega_1) + S_{\eta\alpha_1^o}(\omega+\omega_1)S_{\alpha_1^o\eta}(-\omega_1)\} \\
& + \Gamma^1_{1\alpha\alpha}(\omega_1, \omega+\omega_1)\bar{\Gamma}^1_{1\psi\psi}(\omega_1, \omega+\omega_1)\{S_{\alpha_1^o\psi_1^o}(\omega_1)S_\eta(\omega+\omega_1) \\
& + S_{\alpha_1^o\psi_1^o}(\omega+\omega_1)S_\eta(\omega_1) + S_{\eta\psi_1^o}(\omega_1)S_{\alpha_1^o\eta}(\omega+\omega_1) + S_{\eta\psi_1^o}(\omega+\omega_1)S_{\alpha_1^o\eta}(\omega_1)\} \\
& + \Gamma^1_{1\alpha\psi}(\omega_1, \omega+\omega_1)\bar{\Gamma}^1_{1\psi\alpha}(\omega_1, \omega+\omega_1)\{S_{\psi_1^o\alpha_1^o}(\omega_1)S_\eta(\omega+\omega_1) \\
& + S_{\psi_1^o\alpha_1^o}(\omega+\omega_1)S_\eta(\omega_1) + S_{\eta\alpha_1^o}(\omega_1)S_{\psi_1^o\eta}(\omega+\omega_1) + S_{\eta\alpha_1^o}(\omega+\omega_1)S_{\psi_1^o\eta}(\omega_1)\}
\end{aligned}
$$

$$+ \Gamma^1_{1\psi\alpha}(\omega_1, \omega+\omega_1)\bar{\Gamma}^1_{1\psi\psi}(\omega_1, \omega+\omega_1)\{S_{\psi_1^0}(\omega_1)S_\eta(\omega+\omega_1)$$
$$+ S_{\psi_1^0}(\omega+\omega_1)S_\eta(\omega_1) + S_{\eta\psi_1^0}(-\omega_1)S_{\psi_1^0\eta}(\omega+\omega_1) + S_{\eta\psi_1^0}(\omega+\omega_1)$$
$$\times S_{\psi_1^0\eta}(-\omega_1)\} + \Gamma^1_{1\alpha\beta}(\omega_1, \omega+\omega_1)\bar{\Gamma}^1_{1\psi\beta}(\omega_1, \omega+\omega_1)\{S_{\beta_1^0}(\omega_1)S_\eta(\omega+\omega_1)$$
$$+ S_{\beta_1^0}(\omega+\omega_1)S_\eta(\omega_1) + S_{\eta\beta_1^0}(-\omega_1)S_{\beta_1^0\eta}(\omega+\omega_1) + S_{\eta\beta_1^0}(\omega+\omega_1)$$
$$\times S_{\beta_1^0\eta}(-\omega_1)\}]\,\mathrm{d}\omega_1. \tag{A2}$$

## APPENDIX B: THE EXPRESSIONS FOR THE NEW NONLINEAR FORCE TRANSFER FUNCTIONS $\Gamma_{\alpha\psi}$ and $\Gamma_{\psi\alpha}$ FOR A BOTTOM-MOUNTED CYLINDER

In this appendix, the semi-analytical expressions for the new nonlinear force transfer functions $\Gamma_{\alpha\psi}$ and $\Gamma_{\psi\alpha}$ defined in equations (48) and (49) are given for a bottom-mounted cylinder of radius $R$ in water of depth $h$.

The scattered potential $\varphi_s$ for a wave of amplitude $a$ (MacCamy & Fuchs 1954), and the radiation potentials for surge (amplitude $\alpha$) $\varphi_\alpha$ and pitch (amplitude $\psi$) $\varphi_\psi$ (Petrauskas 1976) for a bottom-seated cylinder are given by

$$\varphi_s = \frac{\mathrm{i}ga}{\omega}\sum_{n=-\infty}^{\infty} f_n(m_0 r)\xi_0(m_0 z)\cos(n\theta),$$

$$\varphi_\alpha = \alpha_t[G_0^\alpha(m_0 r)\xi_0(m_0 z) + \sum_{j=1}^{\infty} G_j^\alpha(m_j r)\xi_j(m_j z)]\cos\theta,$$

$$\varphi_\psi = \psi_t[G_0^\psi(m_0 r)\xi_0(m_0 z) + \sum_{j=1}^{\infty} G_j^\psi(m_j r)\xi_j(m_j z)]\cos\theta,$$

where

$$f_n(m_0 r) = (-\mathrm{i})^n[J_n(m_0 r) - \frac{\mathrm{J}'_n(m_0 R)}{\mathrm{H}_n^{(2)'}(m_0 R)}\mathrm{H}_n^{(2)'}(m_0 r)],$$

$$G_0^\alpha(m_0 r) = \frac{4\sinh(m_0 h)\cosh(m_0 h)}{m_0\{2m_0 h + \sinh(2m_0 h)\}}\frac{\cosh\{m_0(z+h)\}}{\cosh(m_0 h)}\frac{\mathrm{H}_1^{(2)}(m_0 r)}{\mathrm{H}_1^{(2)'}(m_0 R)},$$

$$G_j^\alpha(m_0 r) = \frac{4\sin(m_j h)\cos(m_j h)}{m_j\{2m_j h + \sin(2m_j h)\}}\frac{\cos\{m_j(z+h)\}}{\cos(m_j h)}\frac{\mathrm{K}_1(m_j r)}{\mathrm{K}'_1(m_j R)},$$

$$G_0^\psi(m_0 r) = \frac{4\{m_0 h\sinh(m_0 h) - \cosh(m_0 h) + 1\}}{m_0^2\{2m_0 h + \sinh(2m_0 h)\}}\frac{\cosh(m_0 h)\cosh\{m_0(z+h)\}}{\cosh(m_0 h)}\frac{\mathrm{H}_1^{(2)}(m_0 r)}{\mathrm{H}_1^{(2)'}(m_0 R)},$$

$$G_j^\psi(m_j r) = \frac{4\{m_j h\sin(m_j h) + \cos(m_j h) - 1\}}{m_j^2\{2m_j h + \sin(2m_j h)\}}\frac{\cos(m_j h)\cos\{m_j(z+h)\}}{\cos(m_j h)}\times\frac{\mathrm{K}_1(m_j r)}{\mathrm{K}'_1(m_j R)},$$

$$\xi_0(m_0 z) = \frac{\cosh\{m_0(z+h)\}}{\cosh(m_0 h)}, \qquad \xi_j(m_j z) = \frac{\cos\{m_j(z+h)\}}{\cos(m_j h)}.$$

In these expressions, $\mathrm{H}_n^{(2)}(m_0 r)$ is the Hankel function of the second kind of order $n$, and $\mathrm{K}_1$ is the modified Bessel function of the second kind of order one. Following the solution procedure described in Drake *et al.* (1984), the semi-analytical expression for the new transfer function $\Gamma_{\alpha\psi}$ is given by

$$\frac{\Gamma_{\alpha\psi}(\omega,\omega)}{\frac{1}{2}\rho g\pi R} = -(\bar{f}_0 + \bar{f}_2)\frac{\omega^2}{g}\sum_{j=0}^{\infty} G_j^\psi + \frac{2\bar{f}_2}{R^2}G_0^\psi I_1^\alpha + (\bar{f}_0 + \bar{f}_2)\left(G_0^\psi I_2^\alpha + \sum_{j=1}^{\infty} G_j^\psi\right)$$
$$- \frac{2}{m_0 R}\bar{f}_2\frac{m_0 h\sinh(m_0 h) - \cosh(m_0 h) + 1}{m_0\cosh(m_0 h)}, \tag{B1}$$

where

$$I_1^\alpha = \frac{\omega^2}{2gm_0^2}\left(1 + \frac{2m_0h}{\sinh(2m_0h)}\right), \qquad I_2^\alpha = \frac{1}{2}\left(1 - \frac{2m_0h}{\sinh(2m_0h)}\right).$$

Following a similar approach, the expression for transfer function $\Gamma_{\psi\alpha}$ is derived as

$$\frac{\Gamma_{\psi\alpha}(\omega,\omega)}{\frac{1}{2}\rho g\pi R} = -h(\bar{f}_0 + \bar{f}_2)\frac{\omega^2}{g}\sum_{j=0}^{\infty} G_j^\alpha + \frac{2\bar{f}_2}{R^2}\left(G_0^\alpha I_1^\psi + \sum_{j=1}^{\infty} G_j^\alpha I_2^\psi\right)$$
$$+ (\bar{f}_0 + \bar{f}_2)\left(G_0^\alpha I_3^\psi + \sum_{j=1}^{\infty} G_j^\alpha I_4^\psi\right) - \frac{2}{m_0R}\bar{f}_2\frac{m_0h\sinh(m_0h) - \cosh(m_0h) + 1}{m_0\cosh(m_0h)}, \tag{B2}$$

where

$$I_1^\psi = \int_0^h z\xi_0^2\,\mathrm{d}z, \qquad I_2^\psi = \int_0^h z\xi_0\xi_j\,\mathrm{d}z,$$
$$I_3^\psi = \int_0^h z\left(\frac{\partial\xi_0}{\partial z}\right)^2\mathrm{d}z, \qquad I_4^\psi = \int_0^h z\frac{\partial\xi_0}{\partial z}\frac{\partial\xi_j}{\partial z}\,\mathrm{d}z.$$

As mentioned above, $\Gamma_{\alpha\psi}$ and $\Gamma_{\psi\alpha}$ must satisfy the reciprocity relation. It can readily be noticed that the last terms of equations (B1) and (B2) are identical. But the agreement between the remaining terms in the expressions for $\Gamma_{\alpha\psi}$ and $\Gamma_{\psi\alpha}$ (given in equations (B1) and (B2)) is less apparent. However, the very close similarity of these remaining terms, and thus the reciprocity requirement, has been checked numerically in Section 6.